Polymer 50 (2009) 189–200

Contents lists available at ScienceDirect

Polymer

journal homepage: www.elsevier.com/locate/polymer

Electrospinning of chitosan–poly(ethylene oxide) blend nanofibers in the presence of micellar surfactant solutions

C. Kriegel [a], K.M. Kit [b], D.J. McClements [a], J. Weiss [a,*]

[a] Department of Food Science, University of Massachusetts, Chenoweth Laboratory, 100 Holdsworth Way, Amherst, MA 01003, USA
[b] Department of Materials Science and Engineering, University of Tennessee, 434 Dougherty Engineering Building, Knoxville, TN 37996, USA

ARTICLE INFO

Article history:
Received 26 July 2008
Received in revised form
14 September 2008
Accepted 21 September 2008
Available online 2 October 2008

Keywords:
Electrospinning
Chitosan
Poly(ethyleneoxide)

ABSTRACT

Nanofibers were fabricated by electrospinning a mixture of cationic chitosan and neutral poly(ethylene oxide) (PEO) at a ratio of 3:1 in aqueous acetic acid. Chitosan ((1 → 4)-2-amino-2-deoxy-β-D-glucan) is a multifunctional biodegradable polycationic biopolymer that has uses in a variety of different industrial applications. Processing conditions were adjusted to a flow rate of 0.02 ml/min, an applied voltage of 20 kV, a capillary tip-to-target distance of 10 cm and a temperature of 25 °C. To further broaden the processing window under which nanofibers are produced, surfactants of different charge were added at concentrations well above their critical micellar concentrations (cmc). The influence of viscosity, conductivity and surface tension on the morphology and physicochemical properties of nanofibers containing surfactants was investigated. Pure chitosan did not form fibers and was instead deposited as beads. Addition of PEO and surfactants induced spinnability and/or yielded larger fibers with diameters ranging from 40 nm to 240 nm. The presence of surfactants resulted in the formation of needle-like, smooth or beaded fibers. Compositional analysis suggested that nanofibers consisted of all solution constituents. Our findings suggest that composite solutions of biopolymers, synthetic polymers, and micellar solutions of surfactants can be successfully electrospun. This may be of significant commercial importance since micelles could serve as carriers of lypophilic components such as pharmaceuticals, nutraceuticals, antimicrobials, flavors or fragrances thereby further enhancing the functionality of nanofibers.

1. Introduction

Electrospinning is a technique that involves applying a high voltage between the tip of a syringe and a collector plate, with a polymer solution being contained within the syringe. The voltage causes a jet of polymer solution to be expelled from the syringe and move towards the collector plate. As the solvent in the jet dries the remaining polymer solidifies and forms ultrafine nanofibers that are collected on the collector plate as a non-woven mesh or membrane. Electrospinning can produce polymer nanofibers ranging from 10 to several 100 nm in diameter whose properties depend on polymer type, solution properties and processing conditions. To date, a wide variety of polymers and blends of polymers have been electrospun, with synthetic polymers yielding the best results, i.e. fibers of high mechanical strengths and uniform morphologies. The generated nanofibers have very large surface area-to-mass ratios that may sometimes be as high as several 100 m^2/g and may be engineered to have high porosities with small pore size. These properties have led to the development of numerous applications in the field of biomedical engineering [1,2], drug delivery, biosensors, material science, pharmacy and increasingly food science. Fabrication of nanofibers from biopolymers has attracted increased interest due to the fact that biopolymers may have superior biocompatibility and biodegradability, are generally non-toxic, renewable and available at lost costs, and may have functionalities such as antioxidant, antimicrobial or enzyme activities [3]. However, electrospinning of nanofibers from biopolymers has proven to be challenging because they have limited solubility in most organic solvents, are often polyelectrolytes when dissolved, have poor molecular flexibilities, readily form three-dimensional networks via hydrogen bonds, and most importantly are insufficiently entangled to facilitate electrospinning [4].

Chitosan, a copolymer of (1 → 4)-2-amino-2-deoxy-β-D-glucan and (1 → 4)-2-acetamido-2-deoxy-β-D-glucan, capable of forming extensive intra- and intermolecular hydrogen bonds can be derived from chitin, one of the most abundant biopolymers, by

* Corresponding author. Department of Food Science and Biotechnology, University of Hohenheim, Garbenstrasse 25, 70599 Stuttgart, Germany. Tel.: +49 711 459 23292; fax: +49 711 459 23233.
E-mail address: j.weiss@uni-hohenheim.de (J. Weiss).

0032-3861/$ – see front matter © 2008 Elsevier Ltd. All rights reserved.
doi:10.1016/j.polymer.2008.09.041

deacetylation in NaOH [5,6]. At pH below its pKa, chitosan behaves like a cationic polyelectrolyte. Chitosan molecules carry a high positive charge density due to the protonation of the amino groups attached to their backbone. The positive charge of chitosan gives rise to a number of useful functional properties. For example, chitosan may bind free fatty acids during digestion of fatty meals thereby preventing adsorption making it of interest to manufacturers of dietary weight loss supplements [7,8]. In the food industry, its broad spectrum of antimicrobial activity against yeasts, fungi and bacteria have resulted in being investigated as a novel, naturally-occurring food preservative [9–12]. Production of nanofibers from chitosan may thus enable the development of novel food, pharmaceutical, and cosmetic applications.

Electrospinning of chitosan has been investigated by several authors all of which found that the manufacture of pure chitosan nanofibers was extremely challenging [13–18]. Some authors reported success in electrospinning homogeneous chitosan nanofibers from chitosan solutions of relatively high concentration and low molecular weight upon dispersion in solvents such as trifluoroacetic acid [19], 1,1,1,3,3,3-hexafluoro-2-propanol [20] where further extraction of the solvent became necessary or concentrated aqueous acetic acid [21,22]. Unfortunately, low molecular weight chitosans have shown to exhibit lower biological activities and the presence of residues of the above mentioned solvents may prohibit their application in food systems.

Researchers have instead focused on electrospinning blends of chitosan with other compatible polymers such as PVA [16,18,23,24], PEO [13,25,26], or others [27]. In blends, the fiber forming ability of the co-spinning agent is utilized to facilitate polymer entanglement and generation of a polymer jet. Electrospinning of polymer blends is also an efficient way to create composite nanofibers that have improved material properties such as higher tensile strengths. Based on previous studies, we chose to use poly(ethylene oxide) as a co-spinning agent due to its excellent electrospinning characteristics, its ability to form ultrafine fibers, its linear structure with flexible chains, its biocompatibility, its solubility in aqueous media, and its capability to form hydrogen bonds with other macromolecules. In a chitosan–PEO blend, PEO acts as a plasticizer facilitating orientation and flow of chitosan by uncoiling and wrapping around chitosan chains [28].

Surfactants are used in a wide array of applications because of their potential to lower surface or interfacial tension of the medium in which they are dissolved [29]. Each molecule contains both a hydrophilic and a hydrophobic part. An ionic surfactant, which has an ionic hydrophilic head, may also improve the electrical conductivity of the solution, promoting bending instability during the electrospinning process, thereby facilitating thinner fiber production with a higher degree of orientation [30]. Further, surfactants may self-assemble to form colloidal aggregates above a critical concentration, the so-called critical micellar concentration or cmc [31]. These micellar solutions are able to serve as solubilization vesicles to improve solubility and protect and deliver lypophilic functional ingredients. Incorporation of micelles into nanofibers could thus offer a novel means to further functionalize biopolymer nanofibers and their blends. Finally, polymer–surfactant interactions may modulate the molecular structure and interactions of polymer molecules thereby altering rheological and interfacial properties of polymer dispersions [30], which are critical factors in the successful preparation of nanofibers by electrospinning. For example, addition of small amounts of nonionic surfactant was found to improve both the onset voltage and the reproducibility of electrospinning [32]. In nonionic polymer solutions, nonionic surfactants did not stop bead formation but greatly reduced it, while cationic surfactants prevented beaded fibers and lead to fibers with smaller mean diameters [30].

In this study, we hypothesize that addition of surfactants to polymer solutions may prove to be a convenient means to (a) modulate the electrospinning conditions of biopolymer–polymer blends and (b) further functionalize fibers by either altering surface properties of fibers or by inclusion of micellar structures that could serve as vehicles for lypophilic functional ingredients. To test this hypothesis, various surfactants (anionic, cationic and nonionic) were added to chitosan–PEO solutions. Solutions were subjected to electrospinning and the influence of surfactant type and charge on solution properties and on the size and morphology of the nanofibrous structures generated were evaluated.

2. Materials and methods

2.1. Materials

Chitosan derived from shrimp shells was obtained from Primex (Reykjavik, Iceland) in the form of flakes. As stated by the manufacturer, the viscosity of a 1 wt% chitosan solution (in 1 wt% acetic acid) was 569 cP ($M_w \sim 1000$ kDa) and the degree of deacetylation was 80%. Poly(ethylene oxide) (PEO) (Cat #343) with a molecular weight of 900 kDa was purchased from Scientific Polymer Products, Inc. (Ontario, NY, USA). Glacial acetic acid (CAS #64197, UN 2789) was purchased from Acros Organics (Morris Plains, NJ, USA). Anionic sodium dodecyl sulfate (SDS) (#71729) was obtained from Fluka, nonionic polyoxyethylene glycol (23) lauryl ether (Brij 35) (#P1254) from Sigma, and cationic dodecyltrimethylammonium bromide (DTAB) (CAS #1119944) from Acros Organics (see above). The critical micellar concentrations were 2.3 mM, 0.09 mM and 14 mM for SDS, Brij 35 and DTAB, respectively [33]. All reagents were used as received from the manufacturer without further purification.

2.2. Methods

2.2.1. Preparation of surfactant–polymer solutions

Solutions were prepared with distilled and deionized water and reagent grade glacial acetic acid. Concentrations of all polymer solutions are in wt/wt% except where noted otherwise. Chitosan–PEO solutions with total polymer concentrations of 1.6% were prepared by dissolving chitosan and PEO in 50 and 90% acetic acid at ratios of chitosan to PEO of 1:0, 3:1 and 0:1. Solutions containing surfactants and polymers above their critical micellar concentrations were obtained by dissolving 2 mM Brij 35, 10 mM SDS, or 36 mM DTAB (which corresponds to a concentration of approximately twice the cmc) in aqueous acetic acid followed by addition and dissolution of chitosan and PEO. Additional controls consisted of 0.4% and 1.2% PEO and chitosan solutions in 50 and 90% acetic acid, respectively. These concentrations were selected because they comprise the individual polymer solutions in the chitosan–polymer blend. All solutions were kept under constant stirring for 8 h at 25 °C to ensure complete dissolution of the polymers and to obtain homogeneous solutions. All solutions were then used immediately for electrospinning.

2.2.2. Electrospinning of solutions

The schematic setup and photographic image of the equipment used in this study are shown in Fig. 1. 20 ml of polymer dispersions were placed in a 20-ml syringe (Micro-Mate, Popper & Sons, New Hyde Park, NY, USA) that had a 0.69 mm diameter stainless steel capillary (Hamilton, NE, USA No. 91019) with a blunt tip. The syringe was placed in a syringe pump (Harvard apparatus; 11plus, Holliston, MA, USA) which permitted adjustment and control of solution flow rates. The metal capillary of

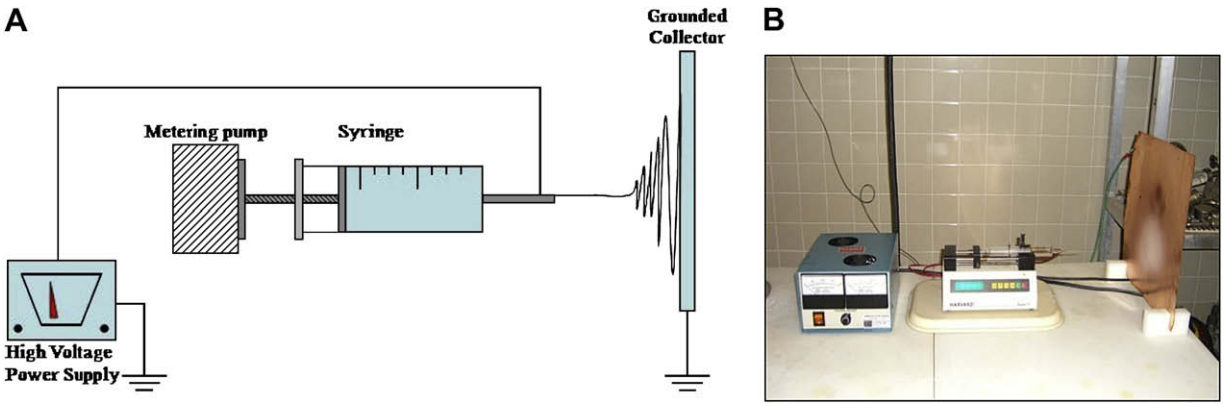

Fig. 1. (A) Schematic illustration and (B) photographic image of the electrospinning setup used in this study.

the syringe was connected to the positive lead of a high voltage power supply (Gamma High Voltage; ES 30P-5 W, Ormond Beach, FL, USA), operated in positive DC mode that could generate voltages up to 30 kV. A grounded copper plate wrapped in aluminum foil and mounted onto two polypropylene blocks was used as the target collector plate for collection of fibers and/or beads. The target was placed 10 cm from the capillary tip. The syringe pump delivered polymer solution at a controlled flow rate of 0.02 ml/min, while the voltage was maintained at 20 kV and the temperature at 25 °C. These conditions were kept constant throughout all experiments.

2.2.3. Solution viscosity

Solution viscosity was measured with an oscillatory rheometer with a double co-axial cup and bob measurement system: bob length = 40 mm, diameter = 26.66 mm, and gap width = 0.225 mm (MCR 300, Paar Physica, NJ, USA). The shear stress σ (Pa) of solutions was recorded as a function of shear rate (s^{-1}) at shear rates ranging from 10^{-3} to 10^{3} s^{-1}. Solutions were equilibrated to 25 °C prior to all measurements using a Peltier system. Reported results are averages of triplicate measurements. Measurements were fitted to the power law model [34]:

$$\sigma = K\dot{\gamma}^{n} \tag{1}$$

where K is the consistency coefficient and n is the flow behavior index. If the flow behavior index n equals 1, the solution behaves as a Newtonian fluid; if the index is smaller than 1, the solution exhibits shear thinning, and if the index is larger than 1, the solution is a shear thickening fluid.

2.2.4. Solution conductivity

Electrical conductivity of the polymer solutions was determined using a microelectrophoresis instrument (NanoZS, Malvern Instruments, Worcestershire, UK). The temperature was adjusted to 25 °C prior to the measurements. Reported results are averages of triplicate measurements.

2.2.5. Solution surface tension

The surface tension of each polymer solution was determined using a digital tensiometer (Model K10ST, Kruss USA, Nazareth, PA) based on the Wilhelmy plate method [34]. 40 g of the solutions were poured into a 70 mm diameter glass beaker which was previously rinsed with absolute ethanol and deionized and double distilled water and dried at 70 °C overnight to remove any surface-active material. Solutions were then equilibrated to 25 °C and the platinum plate was lowered into the dispersion to form a meniscus. The surface tension σ was calculated in mN/m from the force F acting on the platinum plate using equation (2) where L is the length of the total meniscus (2 × the length + thickness of the plate) and θ is the contact angle.

$$\sigma = \frac{F}{L\cos\theta} \tag{2}$$

Results shown are averages of duplicate measurements and duplicate samples.

2.2.6. Electron microscopy of nanofibrous structures

The morphology of electrospun nanofibers was observed with a field emission scanning electron microscope (FESEM 6320 FXV, JEOL, MA, USA) operated at 5 kV. Nanofibers were electrospun directly onto aluminum SEM stubs which were mounted on the grounded collector plate. After collection of the fibers, samples were sputter coated with Au in a sputter coater (Cressington 108, Cressington, Watford, UK) for 60 s to reduce electron charging effects. Additional coatings were necessary for samples containing DTAB. The average fiber diameter analysis was performed using image analysis software (ImageJ, NIH, USA) from >50 randomly selected fibers for each sample.

2.2.7. Fourier transform infrared spectroscopy

Compositional and chemical characteristics were evaluated by recording infrared spectra of electrospun fibers using a Fourier transform infrared spectrophotometer (Model IR Prestige 21, Shimadzu Corporation, Columbia, MD, USA) with an attenuated total reflection (ATR) unit attached. Samples were mounted on the mirror and each specimen was scanned at operating wavelengths in the range between 4000 and 700 cm^{-1}. Each measurement was composed of an average of 32 scans at a resolution of 4 cm^{-1} using a Bessel apodization. Measurements showed an average of five wavelength scans. IR-Solution (Shimadzu Corporation, Columbia, MD, USA) and Peakfit 4.12 (SeaSolve Software Inc., San Jose, CA, USA) were used to analyze and deconvolute infrared spectra.

2.2.8. Differential scanning calorimetry

Thermal analysis of electrospun fibers was carried out with a differential scanning calorimeter (Model Q100 DSC, TA Instruments, New Castle, DE, USA). Samples of approximately 5 mg were loaded in DSC pans that were closed using a crimping tool. The specimens were equilibrated to 25 °C for 5 min and then heated from 25 to 180 °C at a heating rate of 2 °C/min. The temperature of sample and reference pans was measured as a function of oven temperature to determine heat flow. Results represent an average of four measurements.

3. Results and discussion

3.1. Apparent viscosity of polymer solutions in the presence and absence of surfactants

The apparent viscosity at a shear rate of 100 s^{-1} ($\eta_{a,100}$) of polymer solutions in 50% and 90% acetic acid with or without surfactants (2 mM Brij 35, 10 mM SDS, and 36 mM DTAB) were measured by constant shear rate (Table 1). Apparent viscosities of the two acetic acid solutions were slightly higher than that of water, e.g. $\eta_{a,100}$ (50 and 90% acetic acid) ~0.002 mPa s. The intrinsic viscosity of chitosan in 50% acetic acid more than doubled from 0.56 to 1.15 Pa s when the chitosan concentration was increased from 1.2% to 1.6%, respectively. Increasing the PEO concentration by a factor of four from 0.4% to 1.6% resulted in an 18-fold increase in apparent viscosity from 0.01 to 0.18 Pa s. The composite solution of chitosan–PEO with 1.2% chitosan and 0.4% PEO (3:1 mixing ratio) and a total polymer concentration of 1.6% had an apparent viscosity of 0.88 Pa s. Addition of PEO to chitosan thus reduced solution viscosity compared to solutions that only contained chitosan at the same overall polymer concentration. However, the viscosity of the polymer blend (0.88 Pa s) was larger than the viscosities of the individual polymer solutions of which the blend consisted, e.g. $\eta_{a,100}$(0.4% PEO) = 0.01 mPa s and $\eta_{a,100}$(1.2% PEO) = 0.56 mPa s. In general, addition of surfactants had only little effect on solution viscosity (Table 1), e.g. addition of SDS, Brij 35 and DTAB at the highest respective concentration led to changes in the apparent viscosity of 1.6% chitosan solutions from 1.15 mPa s to 1.28, 1.14 and 1.04 Pa s, respectively. Similar results were found upon addition of surfactants to chitosan–PEO blend solutions or when 90% acetic acid was used as the solvent although apparent viscosities were generally higher using the higher concentrated solvent.

3.2. Flow behavior of polymer solutions in the presence and absence of surfactants

To gain a more in-depth understanding of the rheological behavior of solutions, flow curves were measured over a shear rate range of 10^{-3}–10^{3} s^{-1} and fitted to the power law equation (equation (1)) to calculate the consistency coefficient K and flow behavior index n (Tables 2 and 3). The consistency coefficient K followed similar trends as the apparent viscosity discussed above, for example in 50% acetic acid, K of chitosan solutions increased more than twice from 4.9 to 12.9 as the chitosan concentration increased from 1.2 to 1.6%. With addition of PEO to the solution, K decreased to 8.6 while K of pure PEO was 0.02 and 0.78 for 0.4 and 1.2% PEO, respectively. In 90% acetic acids, K values were generally larger than in 50% acetic acid. The consistency coefficient in the presence of surfactants increased with addition of SDS seemed to increase solution viscosity, while Brij 35 had little effect on solution viscosity, and DTAB decreased solution viscosity.

The flow behavior index n is an indicator whether the solution has a tendency to behave like a shear thinning, shear thickening or Newtonian liquid. All polymer solutions regardless of composition had indices smaller than 1 suggesting a shear thinning behavior. A reduced n is generally an indication for polymer entanglement, which is a fundamental prerequisite for deposition of nanofibers during the electrospinning process. The flow behavior index in 50% acetic acid of chitosan, PEO and chitosan–PEO at a polymer concentration of 1.6% was 0.47, 0.66 and 0.5 respectively. The flow behavior indices of the individual solutions of which the blend was composed (0.4% PEO and 1.2% chitosan) were 0.92 and 0.52, respectively, that is the composite solution was more shear thinning than its individual components by themselves. Interestingly, the flow behavior index n decreased slightly with addition of surfactants, i.e. n varied between 0.44 and 0.47 for all polymer solutions containing surfactants depending on surfactant type suggesting a more pronounced shear thinning effect which could be related to improved polymer entanglement. In 90% acetic acid, all flow indices were generally lower. For example, the flow behavior n of chitosan solutions decreased from 0.44 to 0.37 and 0.35 upon addition of Brij 35 and SDS while in chitosan–PEO blends, the flow indices decreased from 0.44 to 0.43 and 0.32 with Brij 35 and SDS, respectively.

The observed rheological behavior of polymer solutions in the presence of surfactants suggests that polymer–polymer interactions are modulated by the presence of surfactants and the type of solvent in which the polymers are dissolved (e.g. 50% or 90% acetic acid). Chitosan in acetic acid carries a strongly positive charge. Because of this, solutions containing chitosan can thus be expected to interact electrostatically with ionic surfactants such as SDS and DTAB. Since solutions were added above their critical micellar concentrations, micelles rather than surfactant monomers may interact with the polymer chains. SDS micelles, which are negatively charged, could bind to one or more individual chitosan molecules. This could firstly decrease repulsive interactions between individual chitosan chains facilitating increased entanglement and secondly lead to bridging between polymer chains which may explain the increasing viscosity upon addition of SDS to chitosan and chitosan–PEO blend solutions. DTAB on the other hand is a positively charged surfactant whose head groups should be electrostatically repelled from the cationic groups on the chitosan backbone. Nevertheless, DTAB may still bind to polymers through hydrophobic interactions between its non-polar tail and any non-polar groups on the polymer chain. If binding occurred there would be an increased electrostatic repulsion between chitosan/DTAB complexes thus decreasing entanglement and viscosity. Brij 35 as a nonionic surfactant would be expected to show no electrostatic interaction and instead may interact with polymers solely via hydrophobic binding. The fact that addition of Brij 35 to the polymer solutions caused little change in viscosity suggests that it did not strongly affect the interactions between the polymer molecules.

3.3. Conductivity of polymer–surfactant solutions

Electrical conductivity of polymer–surfactant solutions is shown in Fig. 2. The conductivity of 50% aqueous acetic acid solutions was 0.98 mS/cm whereas that of 90% acetic acid solutions was dramatically lower with only 0.03 mS/cm. At higher

Table 1
Apparent viscosities of polymer–surfactant solutions (50 or 90 wt% Acetic acid).

Polymer Composition		50 wt% Acetic Acid				90 wt% Acetic Acid		
PEO	Chitosan	Buffer	Brij 35	SDS	DTAB	Buffer	Brij 35	SDS
0.4%	–	0.01 ± 0.01				0.02 ± 0.01		
1.6%	–	0.18 ± 0.01	0.17 ± 0.01	0.14 ± 0.01	0.16 ± 0.01	0.27 ± 0.01	0.25 ± 0.00	0.25 ± 0.00
–	1.2%	0.56 ± 0.01				0.61 ± 0.01		
–	1.6%	1.15 ± 0.04	1.14 ± 0.08	1.28 ± 0.01	1.04 ± 0.02	1.15 ± 0.06	1.33 ± 0.18	1.24 ± 0.46
0.4%	1.2%	0.88 ± 0.07	0.89 ± 0.07	0.92 ± 0.14	0.83 ± 0.05	1.04 ± 0.04	0.99 ± 0.06	1.07 ± 0.11

Table 2
Power law consistency coefficient K of polymer–surfactant solutions (50 and 90% Acetic acid).

Polymer Composition		50 wt% Acetic Acid				90 wt% Acetic Acid		
PEO	Chitosan	Buffer	Brij 35	SDS	DTAB	Buffer	Brij 35	SDS
0.4%		0.02 ± 0.01				0.003 ± 0.01		
1.6%		0.78 ± 0.01	0.73 ± 0.01	0.52 ± 0.01	0.64 ± 0.05	1.46 ± 0.14	1.25 ± 0.00	1.26 ± 0.05
	1.2%	4.90 ± 0.11				9.65 ± 0.67		
	1.6%	12.94 ± 0.40	13.83 ± 0.34	16.59 ± 0.34	12.12 ± 0.23	14.5 ± 0.16	24.8 ± 0.35	26.2 ± 0.68
0.4%	1.6%	8.62 ± 1.53	9.63 ± 0.29	13.04 ± 0.32	1.33	14.50 ± 0.10	14.54 ± 2.80	14.54 ± 2.80

concentrations of water in the solution, more molecules can be ionized, and thus a higher conductivity can be attained. Pure PEO solutions had approximately the same level of conductivity as pure acetic acid solutions with 0.99 and 0.03 mS/cm in 50 and 90% acetic acid, respectively. Conductivities of pure chitosan solutions are considerably higher than those of PEO and increase with increasing chitosan concentration. For example, conductivities of 1.6% chitosan were 1.64 and 0.30 mS/cm in 50% and 90% acetic acid, respectively. After blending with PEO, the conductivity of chitosan–PEO solutions decreased due to reduction of the chitosan concentration in the blend, e.g. conductivities of composite solutions were 1.4 and 0.16 mS/cm using 50% and 90% acetic acid, respectively. These conductivities have virtually the same values as the conductivity of the individual chitosan solutions in the blend. For example, a 1.2% chitosan solution had a conductivity of 1.4 and 0.15 in 50% and 90% acetic acid, respectively.

These results are not surprising since chitosan is a polyelectrolyte while PEO is neutral. Generally, the electrical charge of chitosan molecules is primarily determined by their degree of deacetylation (DDA) and solution pH as well as ionic strength [35]. Only deacetylated amino groups can bind protons, thus charge density depends on the degree of deacetylation or the ratio of the two monomers in the chain. A high degree of deacetylation results in a highly charged polycation in acidic solution [36]. The chitosan used in this study was highly deacetylated (>80%) and thus more than 80% of all side groups were theoretically able to carry an electrical charge.

Addition of both SDS and DTAB, the two ionic surfactants further increased the conductivity, while addition of Brij 35, the nonionic surfactant, had no influence on the conductivity of the solutions (Fig. 2). For example, in 50% acetic acid, conductivities of chitosan–PEO blends remained at 1.6 mS/cm after addition of Brij 35 but increased to 1.75 and 2.5 mS/cm when SDS and DTAB, respectively were added. A similar trend was observed in 90% acetic acid with overall conductivities being lower in 90% than in 50% acetic acid, e.g. conductivities of chitosan–PEO blends were 0.16 mS/cm in the absence of surfactants and 0.18 and 0.35 mS/cm after addition of Brij 35 and SDS (conductivities are not listed for DTAB, which could not be dissolved in 90% acetic acid solutions containing chitosan). Results suggest that while addition of ionic surfactants can improve solution conductivity, this effect may be overshadowed by the contribution of the solvent to the conductivity.

3.4. Surface tension

As acetic acid concentration increased from 50% to 90%, surface tension of all solutions without added surfactants decreased from approximately 38 to 30 mN/m (Fig. 3). The presence of any polymer had little influence on the surface tension, i.e. the surface tension of solutions containing no polymer, 1.2–1.6% chitosan or 0.4–1.6% PEO varied between ~37 and 38 mN/m in 50% acetic acid and decreased to ~30–32 mN/m in 90% acetic acid. Upon addition of surfactants, surprisingly little change in surface tension was observed, with exception of addition of SDS in 50% acetic acid, where surface tension significantly decreased to below 30 mN/m. In 90% acetic acid, addition of SDS again had little influence on surface tension, e.g. $\gamma_{chitosan,SDS} = 32.1$ mN/m.

As previously shown, the decrease in surface tension with increasing solvent strength correlated with a decreasing conductivity. In electrospinning, these two opposing effects may somewhat counteract each other as the decreased surface tension will result in lower electric field strengths required for jet initiation [32] while the decreased conductivity will require a higher electric field. In general, both parameters are of key importance to the process of electrospinning influencing whether fibers, beads or bead defects are formed [37]. At higher surface tensions, the reduction of surface areas is increasingly favored due to the increased free energy of the system forcing a breakup of the polymer jets into spheres. On the other hand, higher conductivities may result in increased charge densities being present at the surface of fibers, which may favor an increase in surface area and thus oppose formation of beads and promote thinner jets. Jet breakups favored by surface tension effects are also opposed by viscoelastic forces that resist rapid changes in shape.

The decrease in surface tension upon addition of SDS to a chitosan solution could be explained by the interaction between SDS and chitosan in the solvent. Chitosan may bind to oppositely charged SDS monomers or micelles via electrostatic attractive interaction forces between the polycation and the negatively charged polar group of SDS or SDS micelles [38,39]. In the case of monomers, additional hydrophobic interactions may also favor association of surfactant tails with acetylated patches on chitosan. In contrast, when the polyelectrolyte and surfactants have the same charge (as is the case for chitosan and DTAB), electrostatic repulsions will most likely dominate and associations between polymer and surfactant are weak or non-existing unless the polyelectrolyte is very strongly hydrophobic [40]. Likewise, nonionic surfactants

Table 3
Power law flow behavior index n of polymer–surfactant solutions (50 and 90% Acetic acid).

Polymer Composition		50 wt% Acetic Acid				90 wt% Acetic Acid		
PEO	Chitosan	Buffer	Brij 35	SDS	DTAB	Buffer	Brij 35	SDS
0.4%		0.92 ± 0.01				0.88 ± 0.01		
1.6%		0.66 ± 0.02	0.69 ± 0.00	0.72 ± 0.00	0.70 ± 0.01	0.88 ± 0.01	0.64 ± 0.00	0.64 ± 0.00
	1.2%	0.52 ± 0.01				0.42 ± 0.01		
	1.6%	0.47 ± 0.01	0.46 ± 0.01	0.44 ± 0.01	0.46 ± 0.01	0.44 ± 0.01	0.37 ± 0.01	0.35 ± 0.01
0.4%	1.6%	0.50 ± 0.02	0.48 ± 0.01	0.46 ± 0.01	0.49 ± 0.01	0.44 ± 0.02	0.43 ± 0.01	0.32 ± 0.17

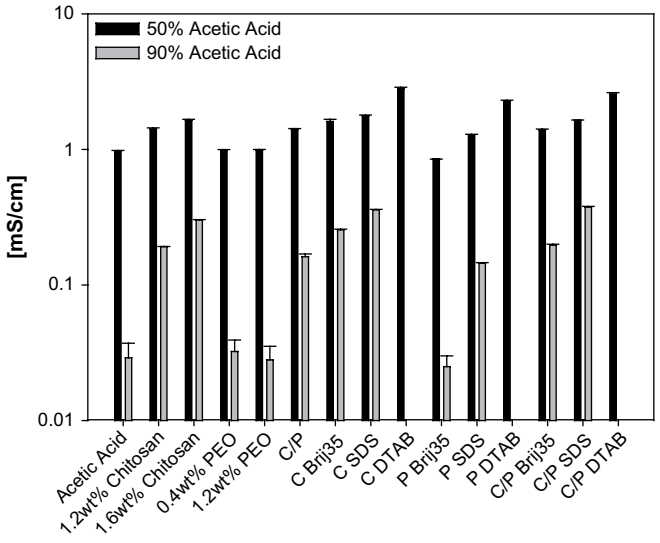

Fig. 2. Electrical conductivity in mS/cm of polymer–surfactant solutions dispersed in 50 and 90% acetic acid.

exhibit low affinity for polyelectrolytes as associations are solely based on hydrogen bonding and/or hydrophobic interactions. This explains the more pronounced effect that SDS had on both solution viscosity and surface tension. As previously noted, chitosan and chitosan–PEO could not be dissolved in DTAB in 90% acetic acid.

3.5. Morphology and fiber diameter

Pure chitosan did not form fibers in either solvent; and beads or drops were instead deposited with a very limited degree of fiber formation (Fig. 3A). This is in agreement with a number of reported studies that showed that electrospinning of chitosan in aqueous solvents was unsuccessful unless another electrospinning-inducing polymer was added [13–18]. It has been suggested that in the case of chitosan or other charged biopolymers such as sodium alginate, the rapid increase in viscosity with increasing polymer concentration causes solutions to become too viscous before a critical polymer concentration required for

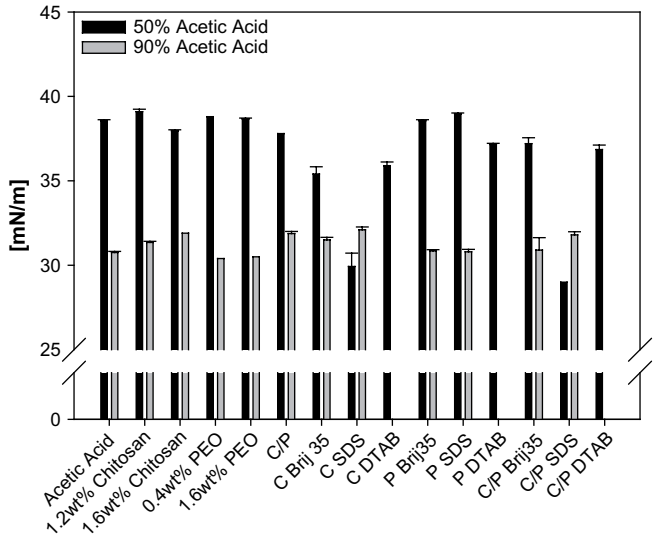

Fig. 3. Surface tension in mN/m of polymer–surfactant solutions dispersed in 50 and 90% acetic acid.

entanglement and formation of fibers can be dissolved in the solvent [3,16].

When surfactants of any type were added to the chitosan solution, the presence of bead defects was not completely prevented but the onset of nanofiber fabrication was greatly improved (Fig. 5C–E). Using Brij 35 (Fig. 5C) resulted in formation of a small amount of ultrafine fibers surrounded by many beads. While we did not test higher concentrations of either surfactant or chitosan in the pure chitosan solutions, bead formation could have potentially been prevented if either concentration had been increased. Further experiments may be required to test this hypothesis. Addition of ionic surfactants to chitosan solutions caused formation of novel nanofibrous structures. In the case of SDS (Fig. 5D), needle-like fibers possibly composed of SDS crystals and chitosan were deposited on the collector plate, while DTAB (E) yielded structures with a beaded-string appearance. In this case the beads could be DTAB micelles that were forced to orient along the surface of the polymer jet during the electrospinning process. Beaded structures were also observed when solutions of pure PEO (1.6 wt%) supplemented with DTAB (36 mM) were electrospun (Fig. 5H). Generally, addition of surfactants did not improve fiber formation of PEO independent of its charge.

Using only PEO at a concentration of 1.6 wt% relatively uniform nanofibers were deposited in 50% acetic acid with rarely any bead defects and very smooth surfaces with no defects in the higher concentrated solvent Fig. 4C and D. Fiber diameters of pure PEO fibers ranged from 70 to 110 nm and from 60 to 230 nm in 50% and 90% acetic acid, respectively. The increased diameter of fibers in the 90% acetic acid could be explained by the decreased conductivity and the increased solution viscosity that decreases whipping and bending instabilities thereby producing fibers with larger diameters and smooth surfaces while in 50% acetic acid fibers had smaller diameter and a somewhat rougher surface. However, using 90% acetic acid as the solvent also resulted in fibers having a broader size distribution [41].

With addition of PEO to chitosan, a well defined Taylor cone was formed, a jet was obtained and a deposition indicative of nanofiber formation was observed at the collector plate surface. FESEM images showed interesting nanofibrous structures with nanofibers having average diameters ranging from 10 to 250 nm. Either solvent was suitable in facilitating the electrospinning and formation of nanofibers from composite solutions without bead defects (Figs. 4F–I and 5A–E). The fiber diameter in the composite fibers was significantly smaller than that of pure PEO fibers and decreased to 30–80 nm using 50% acetic acid and 50–170 nm in 90% acetic acid. The decreased entanglement in the composite solutions may lead to formation of thinner jets that deposit as smaller fibers on the collector plate.

When Brij 35 was added to the polymer blend solutions in 50% acetic acid, smooth nanofibers with diameters varying from 70 to 120 nm were collected (Fig. 5L). Some long and branched fibers were observed which is indicative of the split of a single fiber during the electrospinning process. Addition of SDS to the polymer blends yielded nanofibers of relatively small diameters (10–60 nm), which was the smallest size of nanofibers collected in the experiment, albeit fibers had some minor bead defects. Fiber diameter ranged from 50 to 130 nm in composite samples that contained the positively charged DTAB. We observed additional differences in spun fiber mats not immediately apparent in the SEM images. The fiber mats containing the cationic surfactant DTAB formed very loose spider web or cotton candy like structures rather than the typical; dense paper-like fiber mat depositions that are usually observed for nanofiber membranes (Fig. 6). As previously indicated, we suggest that DTAB accumulated at the surface of fibers giving the fibers a strongly positive overall charge. The individual fibers thus repel each other electrostatically preventing formation of

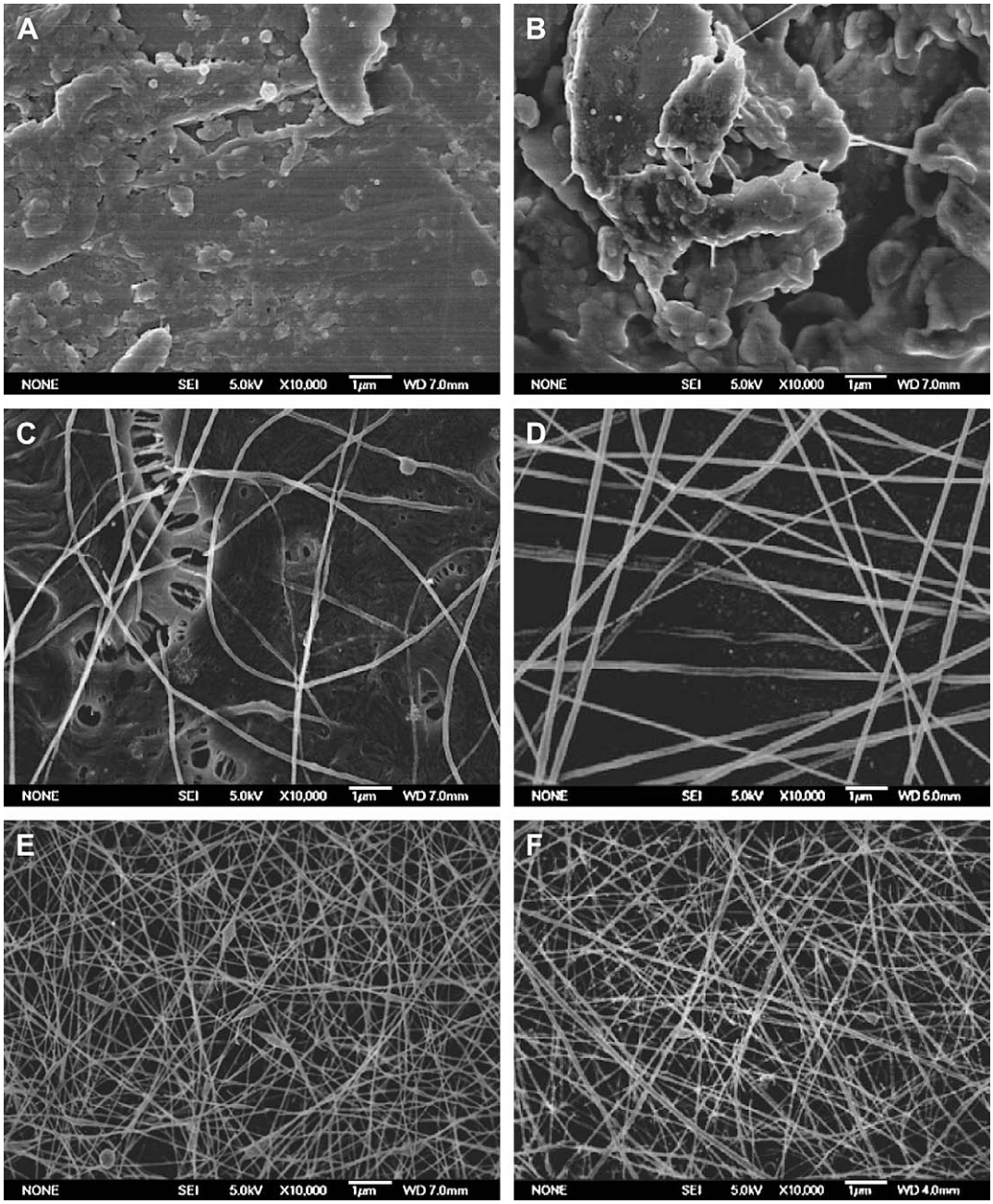

Fig. 4. Scanning electron micrographs of electrospun chitosan, PEO and blends. (A) 1.6 wt% chitosan in 50% acetic acid and (B) 1.6 wt% chitosan in 90% acetic acid; (C) 1.6 wt% PEO in 50% acetic acid (D) 1.6 wt% PEO in 90% acetic acid (E) 1.6 wt% chitosan–PEO (3:1) in 50% acetic acid (F) 1.6 wt% chitosan–PEO (3:1) in 90% acetic acid.

a dense network. Using 90% acetic acid, nanofibers were formed from polymer dispersions supplemented with Brij 35 or SDS. In 90% acetic acid containing the cationic DTAB, it was not possible to dissolve sufficient concentrations of polymer to induce electrospinning. Addition of Brij 35 resulted in nanofibers of a broader diameter ranging from 60 to 250 nm while solutions containing SDS produced fibers with diameters of 70–200 nm. The diameter distribution was very broad and fibers had smooth surfaces. The overall fiber diameter distribution is shown in Table 4.

Our results suggest that the modulation of solution properties (e.g. surface tension, solution viscosity and conductivity) or molecular properties (e.g. conformation and interactions) by addition of surfactants alters the structures that are deposited in the electrospinning process. In particular, interactions of ionic surfactants with solutions containing the polycation chitosan induce alterations in the nanoscalar morphology of fibers as well as the overall structure of the fiber mat produced. This may be explained by the different type of interactions of micellar surfactant solutions with polymers. In principle, three different scenarios are possible when surfactants are mixed with polymers [42–46]:

(1) *Nonionic surfactants and neutral polymers.* Interactions between the two different chemical species are not governed by electrostatic interactions but rather depend on hydrophobic interactions and/or hydrogen bonding. As such, these interactions are weak and only occur if the polymer is sufficiently hydrophobic to facilitate an interaction with the hydrophobic tail of the surfactant. In this case, if surfactants are added below the critical micellar concentration, the hydrophobic part of the amphiphilic surfactant may bind to

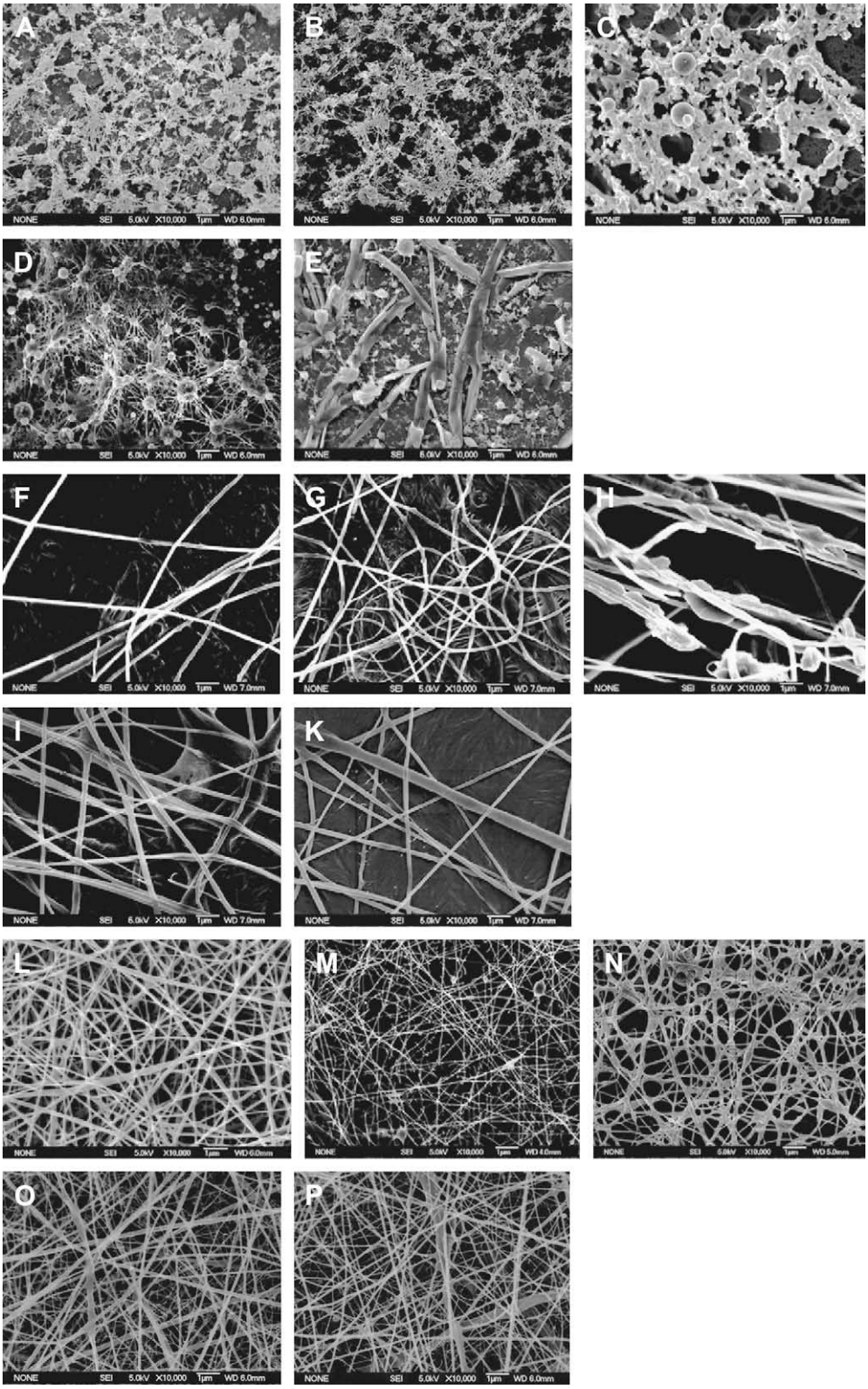

Fig. 5. Scanning electron micrographs of electrospun chitosan (1.6 wt%) with (A) Brij 35 (2 mM) (B) SDS (1 mM) and (C) DTAB (36 mM) in 50% acetic acid. SEM of chitosan (1.6 wt%) in the presence of (D) Brij 35 (2 mM) and (E) SDS (10 mM) in 90% acetic acid. 1.6 wt% PEO nanofibers with (F) 2 mM Brij 35 (G) 1 mM SDS and (H) 36 mM DTAB in 50% acetic acid. SEM micrograph of PEO (1.6 wt%) electrospun with (I) 2 mM Brij 35 and (K) 10 mM SDS in 90% acetic acid. Chitosan–PEO nanofibers (1.6 wt%, ratio 3:1) with (L) 2 mM Brij 35, (M) 1 mM SDS and (N) 36 mM DTAB in 50% acetic acid. Chitosan–PEO electrodepositions with (O) 2 mM Brij 35 and (P) 10 mM SDS in 90% acetic acid.

hydrophobic patches on the polymer thereby leading. Further addition of surfactant on the other hand favors micelle formation as the preferred mechanism of free energy reduction thereby weakening the interaction of the two species. Thus, as observed in our studies, addition of micellar Brij 35 solutions to PEO has little effect on the morphology of electrospun fibers since solution properties except surface tension remain virtually unchanged.

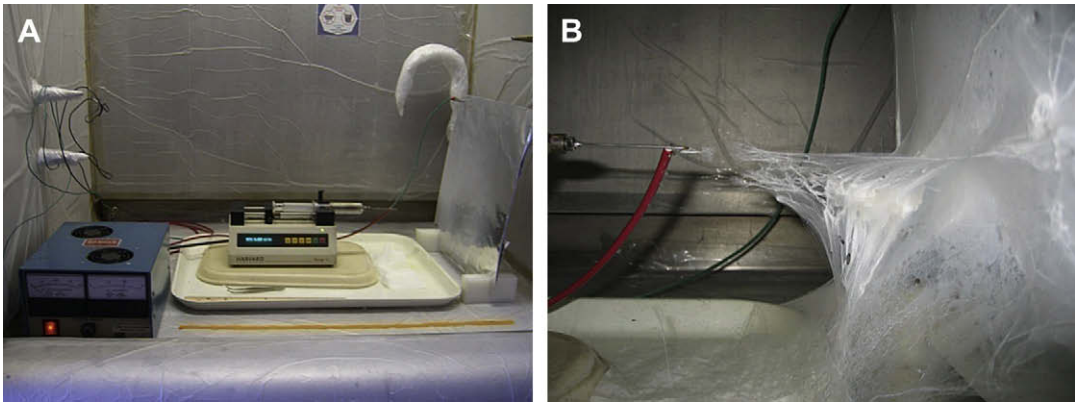

Fig. 6. Photographic image of (A) regular electrospinning setup and (B) electrospinning of chitosan–PEO composite supplemented with the cationic surfactant DTAB.

(2) *Nonionic surfactants and polyelectrolytes or ionic surfactants and neutral polymers.* The nature of this interaction is still somewhat under debate in terms of the specific resulting spatial orientation of polymers and surfactant monomers or micelles [46]. While binding of monomers or surfactants may again be driven by hydrophobic interactions or hydrogen binding, the binding of an uncharged species to a charged one results in a complex that may retain its overall charge thereby affecting intramolecular interactions and conformation of the polymer as well as intermolecular interaction between the complexes. In turn, the polymers may assume a more open structure which could decrease the critical entanglement concentration and thereby facilitate electrospinning. Indeed, addition of Brij 35 to chitosan-containing solutions decreased the onset of fiber production and decreased bead defects.

(3) *Ionic surfactants and charged polymers (polyelectrolytes).* This scenario is quite complex and has thus been the focus of a large number of studies. In this case, electrostatic interactions may govern the overall interaction and introduce substantial changes in solution behavior. If the polymer and the surfactant are oppositely charged, insoluble polymer–surfactant complexes may be formed at lower surfactant concentrations that rapidly phase separate from solution. Here, individual surfactant monomers may bind via their charged headgroup to charged groups on the polyelectrolyte. Conversely, at higher surfactant concentrations, e.g. in micellar surfactant solutions, soluble single phase surfactant–polymer complexes are often formed. Formation of these complexes is driven by both electrostatic attraction and the hydrophobic effect that favor self-aggregation of surfactant monomers. If on the other hand the polymer carries charges of the same sign as the surfactant, the components are typically completely miscible regardless of solution conditions due to the absence of polymer–surfactant or polymer–micelle attractive interactions. Thus, in our studies, the addition of micellar solutions of SDS to solutions containing chitosan may have led to formation of soluble SDS–chitosan coacervates that upon electrospinning created the above described fiber morphology whereas addition of DTAB led to formation of fibers composed of the two blended polymers with micelles accumulated at fiber surfaces.

Table 4
Characteristic properties of fiber deposits shown in Figs. 5 and 6. Denoted are minimum and maximum and average observed diameters as determined by image analysis of Scanning Electron Microscopy images.

Sample	Diameter Range (nm)	Average Fiber Diameter (nm)	Standard Deviation (nm)
C	70–110	99	8.06
D	60–240	141	42.64
E	30–80	55	12.36
F	50–170	123	45.10
L	70–120	94	10.56
M	10–60	39	10.8
N	40–140	92	25.29
O	60–250	151	45.16
P	70–200	139	22.34

Samples C–F correspond to samples C–F in Fig. 5, respectively; samples L–P correspond to samples L–P in Fig. 6, respectively.

3.6. Fourier transform infrared spectroscopy

It has previously been reported that electrospinning of composite solutions may lead to differences in composition of the pre-spun solution and the deposited fibers [34]. For this reason, the composition of deposited fibers was analyzed by infrared spectroscopy. The infrared spectra of cast films and electrospun nanofibers are shown in Fig. 7. Spectra of pure chitosan (which could not be electrospun) were measured on solution-cast films prepared with the same solvents as those used in the electrospinning process. In this case, 20 ml of the solution was cast onto a Petri plate and dried overnight under vacuum to remove the solvent.

Characteristic absorption bands for pure chitosan were observed as follows: a broad band in the range of 3400–3100 cm^{-1} which can be attributed to N–H and OH···O stretching vibrations and intermolecular hydrogen bonding of the polysaccharide molecules [16,47–49]; two middle strong bands at 1655 and 1590 cm^{-1} that may be attributed to the carbonyl C═O–NHR or amide I band and the amine $–NH_2$ or amide II absorption band, respectively [13,47,48]; three peaks at 1380, 1316, and 1255 cm^{-1} assigned to the deformation of $C–CH_3$ and the amide III band [47,49]; and bands at 1150 cm^{-1} showing the anti-symmetric stretching of the C–O–C bridge, at 1060 and 1029 cm^{-1} for skeletal vibrations involving C–O stretching, and at 898 cm^{-1}. These peaks are characteristic for the polysaccharide structure of chitosans [47,48].

Typical absorption bands for PEO were detected at 2885 cm^{-1} and attributed to CH_2 stretching [13,50], but this band overlapped with that observed in chitosan samples. Other characteristic bands were observed at 1148, 1101, 1062, and 958 cm^{-1} assigned to C–O–C stretching vibration [13], and at 1467 cm^{-1} assigned to CH bending, at 1358 and 1340 cm^{-1} assigned to CH deformation of the methyl group, and at 1275, 1240, and 850 cm^{-1}. Since PEO used in the experimental setup had a relatively high molecular weight (900 kDa), the OH absorption bands can be neglected [51]. The OH absorption bands at 3400 and 3100 cm^{-1} are due to stretching vibrations and are thus only attributed to OH within the chitosan polysaccharide chains [51]. With the addition of PEO, the absorbance intensity of CH_2 stretching at 2885 cm^{-1} increased while the

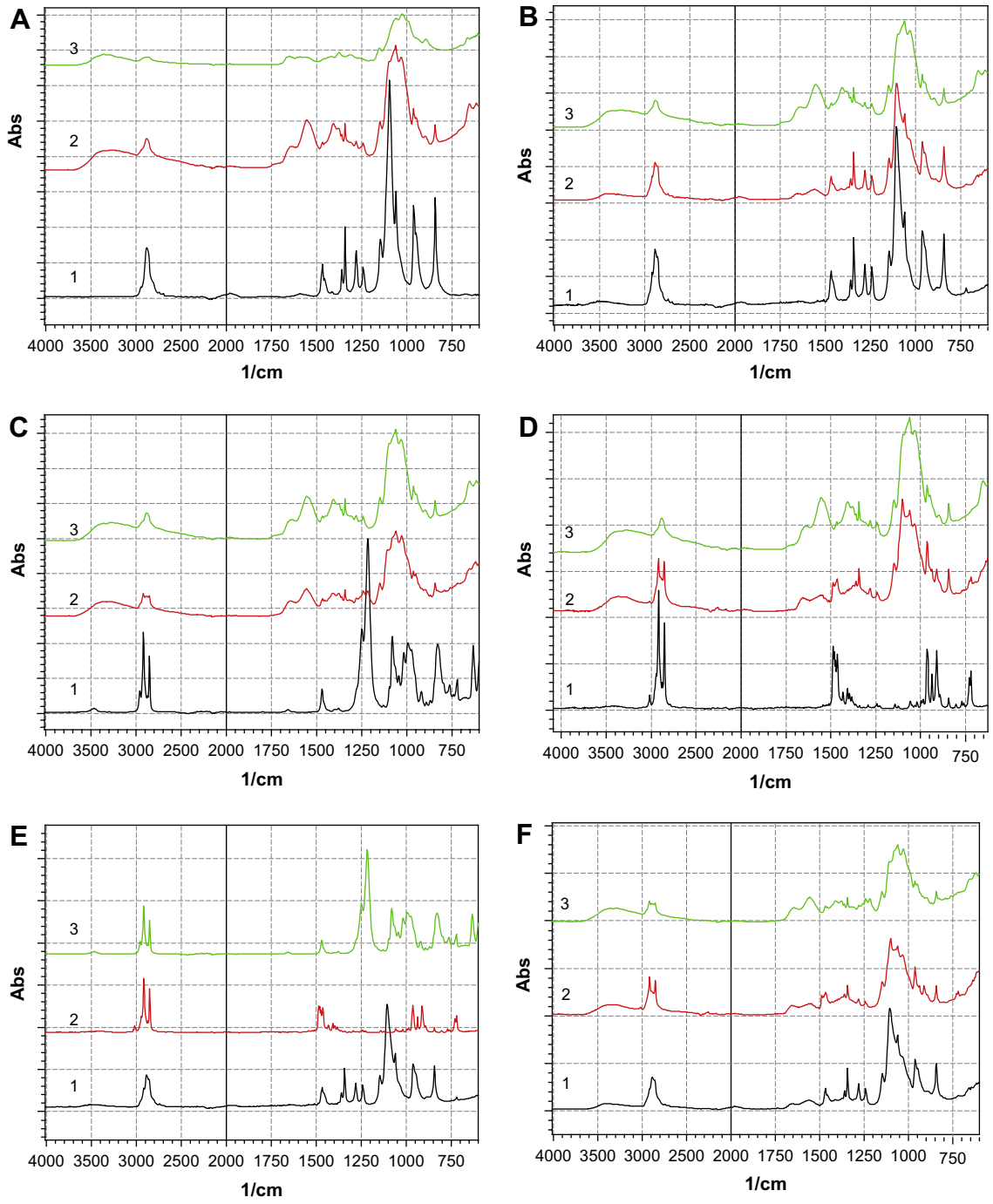

Fig. 7. Infrared absorbance spectra of electrospun chitosan–PEO–surfactant fibers at wave numbers ranging from 4000 to 700 cm^{-1}. (A) spectra of PEO (1), chitosan–PEO fibers (2), and chitosan (3); (B) spectra of pure Brij 35 powder (1), then composite fibers with 2 mM Brij 35 (2) and chitosan–PEO nanofibers (3); (C) spectra of SDS starting with the pure surfactant powder (1) and then composite nanofibers incorporating 10 mM SDS (2) as well as chitosan–PEO electrodepositions (3); (D) spectra of DTAB starting with the pure surfactant powder (1) and then chitosan–PEO nanofibers containing 36 mM DTAB (2) and chitosan–PEO nanofibers (3); (E) spectra of pure surfactant powders of Brij 35 (1), SDS (2) and DTAB (3); (F) comparison of composite nanofiber spectra containing Brij 35 (1), SDS (2) and DTAB (3).

absorbance intensity of $-NH_2$ stretching at around 1590 cm^{-1} decreased.

PEO and the nonionic surfactant Brij 35 have similar structural features and thus have very similar FTIR spectra and absorption bands. Typical bands for DTAB include two strong absorption bands at 2915 and 2850 cm^{-1} attributed to CH_2 methylene stretching vibrations; four medium peaks in the range of 1488–1462 cm^{-1}; and four medium to weak bands between 1430 and 1382 cm^{-1}. In the case of SDS, characteristic bands were observed at 2930, 2847, 1469, and 1184 cm^{-1} assigned to symmetric CH stretching, asymmetric CH stretching, CH bending, and SO stretching, respectively. Characteristic bands for DTAB were observed at 1500, 960, and at 842 cm^{-1}.

Analysis of infrared spectra of chitosan–PEO and chitosan–PEO–surfactant fibers indicated that electrospun nanofibers consisted of all components formerly present in the polymer solution, i.e. no component was selectively excluded during the electrospinning, a fact that is indicative of a successful electrospinning process of all

Table 5
Thermal properties (melting points, transition enthalpies) of polymers and polymer blends in the absence or presence of surfactants in 50% acetic acid. Thermograms of electrospun composite fibers were measured at a scanning rate of 2 °C/min at a temperature range of 25–180 °C.

Samples in 50% Acetic Acid	T_m (°C)	$T_{m,2}$ (°C)	$\Delta H_{m,1}$ (J/g)	$\Delta H_{m,2}$ (J/g)
Chitosan	82.23 ± 3.50	n/a	208.2	n/a
PEO	60.05 ± 1.90	n/a	218.9	n/a
Chitosan–PEO	52.49 ± 0.04	80.85 ± 0.30	24.94	106.4
Chitosan–PEO 2 mM Brij 35	51.16 ± 1.10	74.44 ± 2.91	25.67	48.80
Chitosan–PEO 1 mM SDS	54.64 ± 1.10	76.26 ± 2.83	26.37	48.74
Chitosan–PEO 36 mM DTAB	53.41 ± 0.01	87.53 ± 1.23	29.1	10.64

ingredients. However, addition of any type of surfactant to the chitosan solution led to decrease in intensity of the amide I and II bands while bands characteristic for each of the other ingredients increased in strength. This suggests a decrease in chitosan concentration upon addition of surfactants. Ratios of absorption intensities at 1550 cm^{-1} and 1250 cm^{-1} gave an indication of the relative ratios of chitosan and PEO, respectively. The chitosan concentration in electrospun composite nanofibers in the absence of surfactants was 71% when 50% acetic acid was used and 73.9% when 90% acetic acid was used while the concentration in the polymer solution was 75%. The results were in close agreement with results obtained by thermogravimetric analysis used to verify FTIR analysis (data not shown). Using TGA on the same fibers, the chitosan concentration was determined to be 75% in 90% acetic acid and 72% in 50% acetic acid. When Brij 35 was added to the solution, the chitosan concentration in the fibers decreased to 57.1% using 50% acetic acid and to 21% in 90% acetic acid. A similar trend was observed for the other two surfactants indicating that PEO was preferentially present in the polymer jet. Addition of SDS to the polymer dispersions in 50% acetic acid yielded a chitosan concentration in fibers of 53.5% that decreased to 39% in 90% acetic acid. Using the cationic DTAB as an additive, the chitosan concentration decreased even further to 28%. Thus generally, less chitosan was present in electrospun composite nanofibers if compared with its relative presence in the polymer solutions, indicating that chitosan was less preferentially electrospinnable. This suggests that PEO–chitosan interactions (entanglement) are somewhat reduced by the addition of surfactants.

3.7. Thermal analysis

Finally, electrodepositions were subjected to thermal analysis by differential scanning calorimetry to determine whether surfactants influenced the microstructural features of fibers (e.g. crystallinity) (Tables 5–7). Samples were heated from room temperature to 180 °C and heat flow was measured. Pure chitosan solution-cast films, PEO electrospun nanofibers and surfactants were measured as controls. The majority of polysaccharides do not experience melting but rather degradation upon heating above a certain temperature, which is attributed to their associations through hydrogen bonding [13]. Therefore, their thermograms demonstrated a very broad endothermic transition associated with water evaporation below their characteristic degradation temperature. In the DSC thermogram of chitosan powder, a broad peak occurred at 71.46 ± 1.20 °C. A broadened peak similar to the former also appeared in the thermogram of chitosan–PEO using 50% acetic acid as the common solvent, however, the peak was shifted towards a higher temperature of 81.93 ± 1.94 °C. In the composite fibers, a second peak attributed to PEO was observed at 52.43 ± 0.25 °C, which represents a shift to a lower temperature from the original melting point of PEO at 60.09 ± 0.57 °C in samples composed of 100% PEO. When 90% acetic acid was used, a sharp and intense peak at 64.71 °C ± 0.76 °C for pure PEO fibers was found while two peaks at 60.65 ± 0.43 °C and 78.46 ± 3.50 °C attributed to PEO and chitosan in the composite fibers, respectively, were measured. This shift towards lower melting temperatures with a higher concentration of solvent indicates a higher order in systems containing higher solvent concentrations.

Table 6
Thermal properties (melting points, transition enthalpies) of polymers and polymer blends in the absence or the presence of surfactants in 90% acetic acid. Thermograms of electrospun composite fibers were measured at a scanning rate of 2 °C/min at a temperature range of 25–180 °C. 1 denotes the first observed melting transition upon heating while 2 denotes the second transition.

Samples in 90% Acetic Acid	$T_{m,1}$ (°C)	$T_{m,2}$ (°C)	$\Delta H_{m,1}$ (J/g)	$\Delta H_{m,2}$ (J/g)
Chitosan	71.46 ± 1.20	n/a	208.2	n/a
PEO	64.71 ± 0.76	n/a	158.9	n/a
Chitosan–PEO	60.47 ± 0.43	79.28 ± 4.10	26.21	24.55
Chitosan–PEO 2 mM Brij 35	37.92 ± 0.58	51.93 ± 1.20	70.14	17.64
Chitosan–PEO 10 mM SDS	57.67 ± 0.93	n/a	32.40	n/a

Table 7
Thermal properties of surfactants (melting points, transition enthalpies) measured by differential scanning calorimetry. Thermograms of electrospun composite fibers were measured at a scanning rate of 2 °C/min at a temperature range of 25–180 °C. 1 denotes the first observed melting transition upon heating while 2 denotes the second transition.

Pure surfactants	$T_{m,1}$ (°C)	$T_{m,2}$ (°C)	$\Delta H_{m,1}$ (J/g)	$\Delta H_{m,2}$ (J/g)
DTAB	99.45	n/a	172.8	n/a
SDS	99.83	108.78	2.82	10.85
Brij 35	36.18	138.36	335.7	35.97

Upon addition of the nonionic surfactant Brij 35 using 90% acetic acid as a solvent, the melting points in the composites shifted to 37.92 ± 0.58 and 51.93 ± 1.20 °C. A broad melting peak of chitosan was not observed probably because of the relative higher concentration of surfactant and co-spinning agent. As shown in the FTIR analysis, concentrations of chitosan in the nanofibers decreased with increasing solvent concentration upon addition of surfactants. This could explain why only two endothermic melting transitions were observed, those of Brij 35 and PEO, respectively. Pure Brij 35 powder had two melting endotherms of 36.56 ± 0.54 and 139.25 ± 1.60 °C. Addition of the anionic surfactant SDS resulted in a shift of PEO and the broad chitosan endothermic; the melting points of PEO and chitosan were observed at 57.16 ± 1.07 °C and 75.17 ± 3.02 °C, respectively. Pure SDS had melting transitions at 99.76 ± 0.10 and 106.35 ± 0.44 °C.

When Brij 35 was added to the system containing 50% acetic acid, melting temperatures of 36.56 ± 0.27 °C, 50.76 ± 1.10 and 74.56 ± 2.16 °C for Brij 35, PEO and chitosan, respectively, were observed. Here, the melting point for PEO shifted to a lower temperature as compared to the system in which 90% acetic acid was used. In 50% acetic acid upon addition of the anionic surfactant SDS, T_m for both components shifted to lower temperatures, i.e. 54.64 ± 1.10 and 76.26 ± 2.83 °C for PEO and chitosan, respectively. When the cationic DTAB was added and 50% acetic acid was used as a solvent, two sharp peaks were present. The melting point of PEO was 53.41 ± 0.01 °C and a second peak was observed at 87.86 ± 1.54 °C. Pure DTAB showed a transition at 99.1 ± 0.31 °C.

4. Conclusions

Results of this study demonstrate that addition of surfactants to polymer solutions have a significant influence on the morphology and properties of the generated nanostructures. In particular, if polyionic polymers such as chitosan are to be spun, addition of ionic surfactants alters solution properties such as viscosity, conductivity and surface tension. In turn, these changes in solution properties alter the Taylor cone formation, jet expulsion and jet

bending/whipping, influencing the type, structure and dimensions of the nanostructures formed. In polymer blends composed of a difficult-to-spin biopolymer and a co-spinning agent such as PEO, surfactants may influence entanglement processes. Thus, addition of surfactant can help induce formation of a polymer jet but may simultaneously alter the relative concentration of polymers in the nanofiber generated. Hence, the concentration of one of the polymers in the fibers may be substantially lower than in the original polymer solution. Clearly more studies will be needed to elucidate for example the influence of surfactant concentration upon the electrospinning process. Addition of surfactants above, at or below the critical concentration could alter the generated structures in a variety of ways since in one case, micelles interact with polymer chains while in the other case, surfactant monomers interact with polymer chains. Moreover, the fact that surfactant was co-spun with the blend could make it possible for micelles to remain intact and become part of the nanofibers formed. Since micelles can be loaded with lipophilic functional ingredients, this could serve as an additional means to further functionalize fibers and broaden the number of applications in which nanofibers could be used. We are currently investigating this possibility in an ongoing study.

Acknowledgements

This work was supported by the Environmental Protection Agency Star Grant Program (Grant number: GR832372) and the Massachusetts Experiment Station supported by the Cooperative State Research, Extension, Education Service, United State Department of Agriculture, Massachusetts Agricultural Experiment Station (Projects No. 831 and 911).

References

[1] Reneker DH, Chun I. Nanotechnology 1996;7(3):216–23.
[2] Huang ZM, Zhang YZ, Kotaki M, Ramakrishna S. Composites Science and Technology 2003;63(15):2223–53.
[3] Bhattarai N, Zhang MQ. Nanotechnology 2007;18(45):455601.
[4] Ramakrishna S, Fujihara K, Ganesh VK, Teo WE, Lim TC. Science and engineering of polymer nanofibers. In: Rosenberg KEGaE, ed. Functional nanomaterials; 2006. p. 113–51.
[5] Sorlier P, Denuziere A, Viton C, Domard A. Biomacromolecules 2001;2(3):765–72.
[6] Sugimoto M, Morimoto M, Sashiwa H, Saimoto H, Shigemasa Y. Carbohydrate Polymers 1998;36(1):49–59.
[7] Muzzarelli RAA. Chitin. Pergamon press; 1977.
[8] No HK, Meyers SP, Prinyawiwatkul W, Xu Z. Journal of Food Science 2007;72(5):R87–100.
[9] Zheng LY, Zhu JAF. Carbohydrate Polymers 2003;54(4):527–30.
[10] Je JY, Kim SK. Journal of Agricultural and Food Chemistry 2006;54(18):6629–33.
[11] Helander IM, Nurmiaho-Lassila EL, Ahvenainen R, Rhoades J, Roller S. International Journal of Food Microbiology 2001;71(2–3):235–44.
[12] Rhoades J, Roller S. Applied and Environmental Microbiology 2000;66(1):80–6.
[13] Duan B, Dong CH, Yuan XY, Yao KD. Journal of Biomaterials Science – Polymer Edition 2004;15(6):797–811.
[14] Huang XJ, Ge D, Xu ZK. European Polymer Journal 2007;43(9):3710–8.
[15] Jia YT, Gong J, Gu XH, Kim HY, Dong J, Shen XY. Carbohydrate Polymers 2007;67(3):403–9.
[16] Li L, Hsieh YL. Carbohydrate Research 2006;341(3):374–81.
[17] Spasova M, Manolova N, Paneva D, Rashkov I. E-Polymers 2004.
[18] Zhou YS, Yang DZ, Nie J. Journal of Applied Polymer Science 2006;102(6):5692–7.
[19] Ohkawa K, Cha DI, Kim H, Nishida A, Yamamoto H. Macromolecular Rapid Communications 2004;25(18):1600–5.
[20] Min BM, Lee SW, Lim JN, You Y, Lee TS, Kang PH, et al. Polymer 2004;45(21):7137–42.
[21] Geng XY, Kwon OH, Jang JH. Biomaterials 2005;26(27):5427–32.
[22] De Vrieze S, Westbroek P, Van Camp T, Van Langenhove L. Journal of Materials Science 2007;42(19):8029–34.
[23] Jia YT, Gu XH, Dono FC, Shen XY. Proceedings of 2005 International Conference on Advanced Fibers and Polymer Materials (Icafpm 2005), vols. 1 and 2; 2005. p. 695–99.
[24] Lin T, Fang J, Wang HX, Cheng T, Wang XG. Nanotechnology 2006;17(15):3718–23.
[25] Subramanian A, Lin H-Y, Vu D, Larsen G. Biomed Sci Instrum 2004;40:117–22.
[26] Desai K, Kit K, Li J, Zivanovic S. Biomacromolecules 2008;9(3):1000–6.
[27] Jung KH, Huh MW, Meng W, Yuan J, Hyun SH, Bae JS, et al. Journal of Applied Polymer Science 2007;105(5):2816–23.
[28] Chen ZG, Mo XM, Qing FL. Materials Letters 2007;61(16):3490–4.
[29] Rosen MJ. Surfactants and interfacial phenomenon. Hoboken, NJ: John Wiley & Sons, Inc.; 2004.
[30] Lin T, Wang HX, Wang HM, Wang XG. Nanotechnology 2004;15(9):1375–81.
[31] Neugebauer JM. Methods in Enzymology 1990;182:239–53.
[32] Yao L, Haas TW, Guiseppi-Elie A, Bowlin GL, Simpson DG, Wnek GE. Chemistry of Materials 2003;15(9):1860–4.
[33] Helenius A, McCaslin DR, Fries E, Tanford C. Methods in Enzymology 1979;56:734–49.
[34] Wongsasulak S, Kit KM, McClements DJ, Yoovidhya T, Weiss J. Polymer 2007;48(2):448–57.
[35] Claesson PM, Ninham BW. Langmuir 1992;8(5):1406–12.
[36] Berth G, Dautzenberg H, Peter MG. Carbohydrate Polymers 1998;36(2–3):205–16.
[37] Fong H, Chun I, Reneker DH. Polymer 1999;40(16):4585–92.
[38] Thongngam M, McClements DJ. Journal of Agricultural and Food Chemistry 2004;52(4):987–91.
[39] Thongngam M, McClements DJ. Langmuir 2005;21(1):79–86.
[40] Iliopoulos I, Olsson U. Journal of Physical Chemistry 1994;98(5):1500–5.
[41] Shin YM, Hohman MM, Brenner MP, Rutledge GC. Polymer 2001;42(25):9955–67.
[42] Beheshti N, Zhu K, Kjøniksen A-L, Nyström B. Colloids and Surfaces A: Physicochemical Engineering Aspects 2008;328:79–89.
[43] da Graca-Miguel M. Advances in Colloid and Interface Science 2001;89–90:1–23.
[44] Penfold J, Thomas RK, Taylor DJF. Current Opinion in Colloid & Interface Science 2006;11:337–44.
[45] Thunemann AF. Progress in Polymer Science 2002:1473–572.
[46] Winnik FW, Regismond STA. Colloids and Surfaces A: Physicochemical and Engineering Aspects 2008;118:1–39.
[47] Wan Y, Wu H, Yu AX, Wen DJ. Biomacromolecules 2006;7(4):1362–72.
[48] De Vasconcelos CL, Bezerril PM, dos Santos DES, Dantas TNC, Pereira MR, Fonseca JLC. Biomacromolecules 2006;7(4):1245–52.
[49] Hu Y, Du YM, Yang JH, Tang YF, Li J, Wang XY. Polymer 2007;48(11):3098–106.
[50] Zivanovic S, Li JJ, Davidson PM, Kit K. Biomacromolecules 2007;8:1505–10.
[51] Sawatari C, Kondo T. Macromolecules 1999;32(6):1949–55.